

# MECHANISM NOISE SIGNATURES: IDENTIFICATION AND MODELLING

René Seiler<sup>(1)</sup>, Claudia Allegranza<sup>(2)</sup>

<sup>(1)</sup> ESA/ESTEC, P.O. Box 299, 2200 AG Noordwijk, The Netherlands, E-mail: Rene.Seiler@esa.int

<sup>(2)</sup> AOES B.V., Huygensstraat 34, 2201 DK Noordwijk, The Netherlands, E-mail: Claudia.Allegranza@aoes.com

## ABSTRACT

Many types of space mechanisms, for instance reaction wheel assemblies, scanning systems or solar array drive mechanisms are mission critical items with high requirements on long-term stability of their performance. Therefore, the stable function of key components like ball bearings, gearboxes or electric motors is receiving continuous attention.

While in operation on a spacecraft, the nominally measured feedback from a particular mechanism is often limited to a few telemetry signals with moderate sampling rate. Under such condition, an in-situ diagnosis regarding the state of integral components is very difficult. However, complementary signals might be monitored, in order to get further information on the performance of the particular item, during ground testing or potentially even during a space flight.

Acknowledging earlier work in the relevant areas, it appears promising to dedicate further research to the detection, classification and estimation of mechanism noise signatures for the purpose of health monitoring. The paper addresses the generic problem as well as some typical case studies.

## 1. INTRODUCTION

Space mechanisms for repeated or quasi-continuous operation are often equipped with internal sensors for feedback on their main function, like e.g. the instantaneous rotor speed and motor current of a reaction wheel assembly. However, the activation of a mechanism by an input signal, e.g. an electric current, may also result in a multitude of other responses that can be actually regarded as “unwanted side effects”, for instance mechanical vibration, which might be accompanied by acoustic sound emission under ambient conditions during ground tests. Such effects may be generally considered as “noise” emitted by mechanism.

Various earlier investigations on terrestrial machinery diagnostics and on space equipment, e.g. [1], [2] and [10], suggest that mechanism components and assemblies are generating typical noise signatures during operation. Such noise signatures can be

measured, stored and analysed. In combination with nominal telemetry data, the interpretation of such noise signatures might reveal additional information on the performance and health of individual components and the system as a whole, as well as on the evolution of the performance over time.

Unprocessed mechanism noise data (e.g. resulting from a microvibration characterisation test) tends to be large in size due to, among others, the relatively high sampling rates used and synchronous acquisition of several sensor signals. Hence, for any viable implementation of a health monitoring system, there should be a maximum level of automation in the process covering data acquisition, storage/management and analysis. Therefore, current investigations are focussed on computer-based analysis and the development of the corresponding algorithms.

The discussed approach shall provide some means for obtaining a “noise fingerprint” that can be associated with a specific type of mechanism, and even an individual hardware model. In addition, relevant features in the noise signature of a mechanism should be linked to physical phenomena, where possible. This might enable the equipment suppliers and users to:

- obtain complementary information on the functional performance and status of an individual hardware item (e.g. assessment of design modifications and workmanship),
- compare the behaviour among hardware items of the same type (e.g. establishing an “in-family” vs. “out-of-family” behaviour and related tolerance limits), and
- observe the evolution of a signature over time and over usage for an individual item (e.g. detection of tolerable or non-tolerable changes in performance).

With some future prospect, such approach might allow for non-intrusive monitoring of a mechanism’s condition while it is undergoing a series of ground tests (shock & vibration test, thermal vacuum test, etc.) when intermediate disassembly and inspection of internal components cannot be done. Relating the signatures

obtained on ground with those acquired during flight operation might allow for early intervention in case of an adverse evolution of the performance.

Potentially, in-flight anomaly investigations might be facilitated and improved. In this conjunction, the limited information available via the regular telemetry is judged a severe constraint that can make the identification of physical root causes for a particular in-flight problem extremely difficult. Therefore, the regular monitoring of noise data during spacecraft operation should be reconsidered for future missions with high requirements on the stable performance of long-life mechanisms.

## 2. THE GENERIC PROBLEM

Various aspects may be discussed in a way independent from a specific noise test case or investigation.

The overall process of mechanism noise signature identification and further analysis shall be pursued on the basis of time domain data obtained from suitable sensors (e.g. force transducers or accelerometers) and made accessible via a digital data acquisition system. Signal processing with focus on mechanism noise would normally involving large amount of raw data. Therefore, specific attention has to be given to automation of the entire signal acquisition, management and analysis methodology.

The generic process comprises, among others, the following steps that shall receive specific attention at this stage:

- Data reduction with the aim of condensing relevant information, and extracting characteristic features
- Detection of significant changes, possibly tracking characteristic features over time or with respect to other parameters
- Association of features in the noise signatures with physical phenomena, as far as possible

Regarding the basic structure of relevant noise signatures and the corresponding signal treatment, the following classification shall be applied:

- **Stationary (or quasi-stationary) signals**, including special cases like cyclostationary signals (e.g. generated by reaction/momentum wheel assemblies, continuously operating scanners, etc.). The signal statistics remain constant, or they are only slowly varying over time.
- **Non-stationary signals**, including transient signals (e.g. generated by waveguide switches, valves, piezoelectric motors in pulse driven mode, etc.). The signal statistics may change rapidly.

For **stationary signals**, numerous analysis methods have been established, for instance:

- Time domain: signal statistics, e.g. variance / standard deviation and higher order central moments (skewness and kurtosis), histogram-based estimation of probability density functions, (auto-)correlation function, etc.
- Frequency domain: Power Spectral Density (PSD) and scaled magnitude spectrum of the Fourier transform, considering the effects of spectral averaging and window functions as well as higher order spectra (e.g. bispectrum and trispectrum), etc.
- Further processing for automated feature extraction, e.g. identification and estimation of spectral and order peaks, dedicated filtering, etc.

For **non-stationary signals**, the scope of available analysis tools may be extended by:

- Time-frequency analysis, including Short-Time Fourier Transform, Spectrogram, Wigner-Ville Distribution, Continuous Wavelet Transform & Scalogram, etc.
- Further processing for automated feature extraction, e.g. order analysis, Campbell diagram, etc.

In the following paragraphs, some typical cases using stationary as well as non-stationary noise signals are discussed. All signal processing has been done in MATLAB®.

## 3. THE ON-GROUND TEST CASE

Most individual models of space mechanisms undergo various types of functional tests on ground, as part of development, qualification or acceptance testing. For the discussion of mechanical noise signatures, data acquired in the frame of long-term performance tests (e.g. life testing) and emitted microdisturbance or microvibration tests appear particularly interesting.

In a general case on ground, the test item is connected to drive & control electronics, often in the form of Electrical Ground Support Equipment (EGSE). The test item is stimulated by input signals, and its response is observed via measurable output signals, obtained from internal or external sensors.

For some mechanism equipment, dedicated “mechanical noise” tests are routinely performed, e.g. the characterisation of microdisturbances generated by reaction wheel assemblies. For this purpose, the regular acquisition of telemetry data is accompanied by further (normally external) test sensors and measurement

equipment, for instance to quantify the forces and torques generated at the mechanical interface of the test item.

As the “classical” objective of microvibration tests, the compliance of the mechanism with requirements on maximum allowable disturbances induced on a spacecraft is verified. This kind of mechanical disturbance is more and more becoming a critical issue for high-resolution imaging payloads, e.g. in high-resolution Earth observation spacecraft or space telescopes. Due to their mode of operation, reaction wheel assemblies are (more or less) continuous sources of microdisturbances on a spacecraft. Other equipment with intermittent operation has also been subject of previous investigations; see e.g. in [1], [2] or [9].

However, beyond the “classical” microvibration measurements and analysis with focus on limiting unwanted disturbances at the level of a receiver, e.g. a sensitive payload, the idea of non-intrusive equipment diagnostics and health monitoring on the basis of observing and evaluating microvibration signatures may be pursued.

The measurement of noise signatures directly at equipment level minimises the effect of intermediate structures between noise source and receiver. This approach appears optimal for reference characterisation of a single source on ground. However, it is acknowledged that in many cases it would be impractical (if not impossible) to monitor a noise signature directly at an individual source in flight.

### Case Study:

The characterisation and post-test analysis of mechanical noise created in the form of microvibrations by a set of small reaction wheels has been selected as relevant example.

The on-ground characterisation of microvibration sources at equipment level is rather well established. Typically, the equipment is mounted and operated on a multi-component force measurement platform, i.e. characterised against a known mechanical interface. With a state-of-the-art test bench, the interface forces and torques in all six degrees of freedom are resolved and recorded by means of a digital data acquisition system.

Figure 1 shows a short window of time-history data sampled at 2048 Hz over 8 seconds. It represents the radial force in x-direction measured close to the mounting interface of a small reaction wheel running at 10000 rpm steady-state. The measured signal has been approximately symmetric (mean: 1.4 mN, skewness: 0.035). Nevertheless, for further analysis, a detrending has been applied.

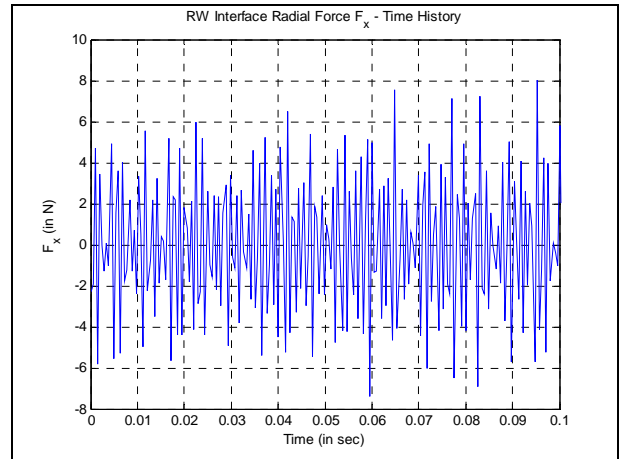


Figure 1: Reaction Wheel No.1 - Radial Force vs. Time

A Root Mean Square (RMS) noise value of about 3.2 N has been found. Furthermore, the noise signature is platykurtic (i.e. sub-Gaussian) with a kurtosis of about 2.2, which appears related to the not dominantly Gaussian random composition of the noise; see also histogram in Figure 2.

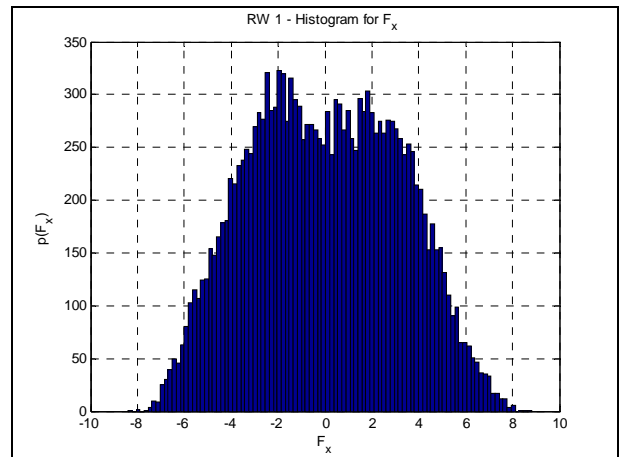


Figure 2: Reaction Wheel No.1 – Noise Histogram

The Power Spectral Density (PSD) of the signal has been obtained using a non-parametric estimator (Welch’s method), with moderate spectral averaging in order to get a high resolution for spectral peaks. The spectrum reveals a whole set of tonal components, see Figure 3.

Wheel speed orders, i.e. integer harmonics of the rotor speed (which is equivalent to about 167 Hz), can be well identified, with magnitudes several orders above the broadband noise. Furthermore, the particular reaction wheel assembly shows tonal features at approximately 1/3 order intervals as well as further narrow-band features at non-integer orders. It should be noted that the broadband levels between the tonal spikes are close to the background noise of the test facility.

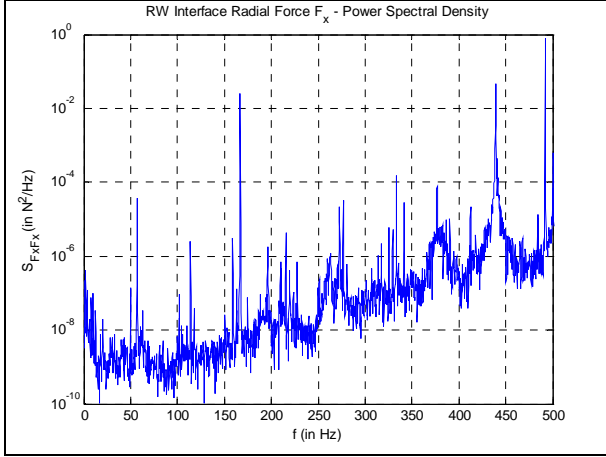


Figure 3: Reaction Wheel 1 - Radial Force  $F_x$  PSD

Figure 4 gives an impression of possible scatter within a group of test items. The scaled magnitude spectra have been plotted over three harmonic orders for four reaction wheel models of the same type (all rotating at 10000 rpm counter-clockwise, *ccw*). Main harmonic components are present with all models. However, with test item 2 the broadband noise level rises significantly above the average of the other items, which might suggest an “out-of-family” behaviour with respect to the noise signature.

For comparison and verification, the equivalent data for the opposite sense of rotation (i.e. clockwise, *cw*) has been plotted in Figure 5. Overall, the spectra are very similar, which is suggesting a “symmetric” behaviour of the hardware with respect to the sense of rotation.

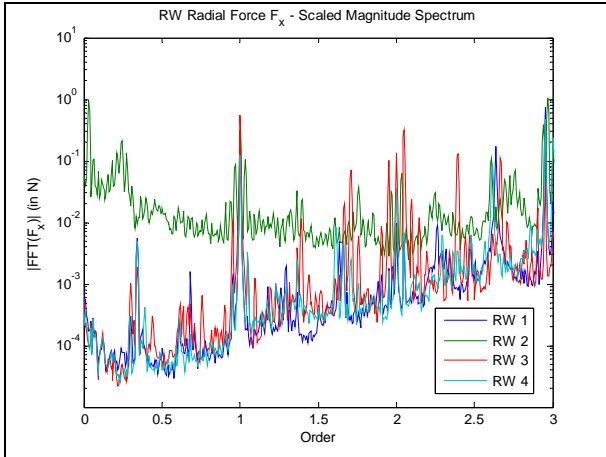


Figure 4: Radial Force  $F_x$  (*ccw*) - Magnitude Spectra

Furthermore, the spectra for the radial forces in orthogonal directions (x and y) have been compared. Figure 4 and Figure 6 are in good agreement with respect to orders and associated magnitudes for all test items.

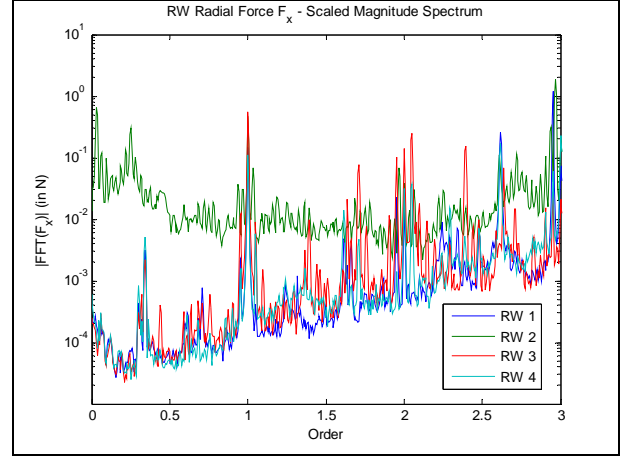


Figure 5: Radial Force  $F_x$  (*cw*) – Magnitude Spectra

However, with Reaction Wheel (RW) 3 the broadband levels in y direction are significantly lower than in x direction, which might be an additional indication on some “out-of-family” behaviour of an individual test item.

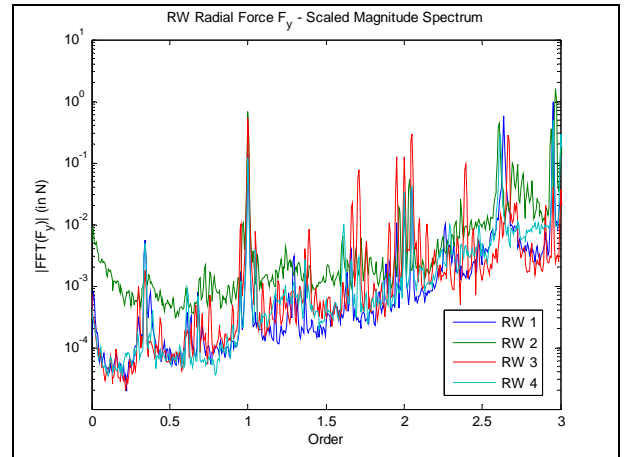


Figure 6: Radial Force  $F_y$  (*ccw*) – Magnitude Spectra

The composite force  $F_h$  due to a set of (integer) harmonic components in the noise signature has been modelled using a Fourier series expansion, truncated to  $N$  relevant harmonics, in the following form (assuming zero mean noise):

$$F_{ih}(t) = \sum_{k=1}^N \hat{F}_k \cdot \cos(k \cdot \omega_{RW} \cdot t - \varphi_k) \quad (1)$$

where  $\hat{F}_k$  ... Amplitude of the k-th harmonic comp.  
 $\varphi_k$  ... Phase of the k-th harmonic comp.  
 $\omega_{RW}$  ... Wheel speed (in rad/s)

The basic harmonic (*H1*) in force and torque signals is largely related to the effects of static and dynamic rotor unbalances, and higher integer order harmonics (*H2*, *H3*, *H4*, *etc.*) may be seen as more complex distortions associated with rotor motion, shaft misalignment, etc.

The contributions by non-integer harmonics may be described in the following general form:

$$F_{nih}(t) = \hat{F}_{nih} \cdot \cos(n_{nih} \cdot \omega_{RW} \cdot t - \varphi_{nih}) \quad (2)$$

where  $\hat{F}_{nih}$  ... Amplitude of the specific component  
 $\varphi_{nih}$  ... Phase of the component  
 $n_{nih}$  ... (Non-integer) Speed factor  
 $\omega_{RW}$  ... Wheel speed (in rad/s)

As addressed by various earlier investigations, e.g. [7], non-integer harmonics might be linked to the relative motion of the individual elements in ball bearings (inner, outer races, balls and retainer) and associated pass frequencies, see also [3]. Furthermore, it has been suggested that play or looseness in the bearing, shaft and housing assembly may result in sub-harmonic components at 1/2 or 1/3 of the shaft speed, see e.g. [10] and [11].

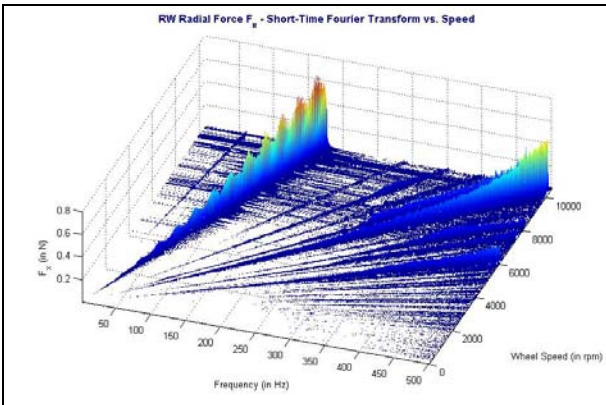


Figure 7: Radial Force  $F_x$  – Scaled STFT Magnitude

Whereas in above considerations only stationary noise signals have been evaluated, reaction wheel microvibrations are commonly recorded while sweeping the entire operational speed range, either via spin-up or coast-down tests. In such cases, analysis methods for non-stationary signals appear more appropriate.

Figure 7 shows the magnitude of the radial force  $F_x$  (scaled in Newtons) of the Short Time Fourier Transform (STFT) plotted over frequency and wheel speed, for a passive coast-down. This type of three-dimensional representation is often referred to as “waterfall plot” (→ harmonic components manifest

themselves as “ray features” converging at the origin). The first and third harmonics (*H1* and *H3*) show the highest magnitudes (it should be noted that the waviness of *H1* is primarily a result of sampling and 3D plotting of the data).

For comparison, the equivalent plot for the orthogonal radial force  $F_y$  is depicted in Figure 8. It can be noticed that the non-integer harmonic *H2.66* is more pronounced than in x-direction.

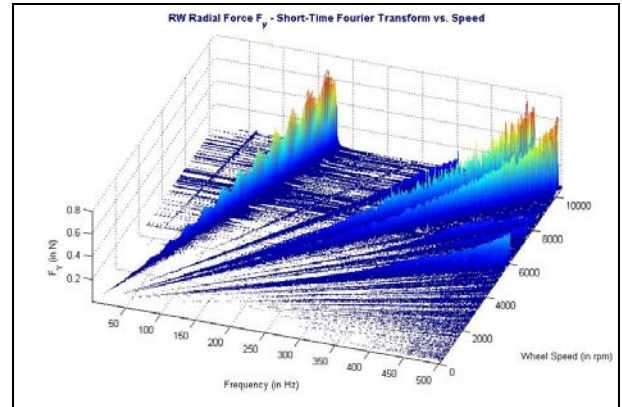


Figure 8: Radial Force  $F_y$  – Scaled STFT Magnitude

With the scope of automated order analysis, the magnitude spectra have been remapped vs. orders, as graphically represented in Figure 9 (→ harmonic components are shown as “parallel line features”).

In this context, it should be noted that orders above *H3* where affected by structural resonances of the test setup, as evident in the right part of the order plot in Figure 9.

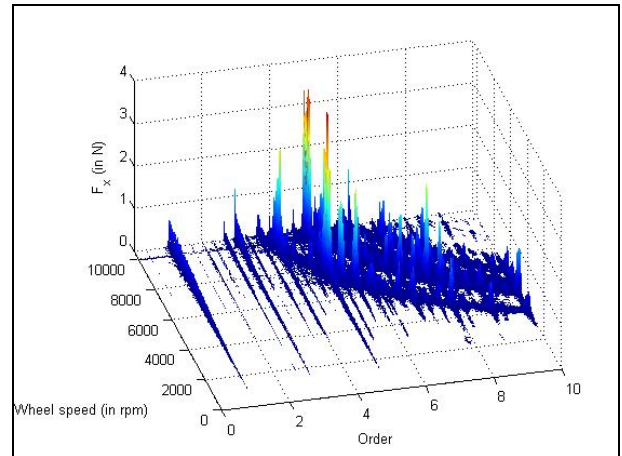


Figure 9: Radial Force  $F_x$  – Order Plot

At this stage, an algorithm for automated local peak detection and order selection based on peak histograms has been applied. This has allowed for separation of individual order components from the rest of the data.

As an extension of the model concept suggested in equations (1) and (2), a statistical model of the type

$$\hat{F}(\omega_{RW}) = a \cdot (\omega_{RW})^b \quad (3)$$

has been fitted to individual order components. *Figure 10* shows the result of a fit for harmonic order *H1*, aiming at a smoothed evolution along the maximum peaks, rather than the least mean square error for all peaks extracted from the spectra.

With the specific reaction wheel assembly considered, the exponent *b* in equation (3) has been estimated with a value of about 1.8, whereas a theoretical value of 2 should be expected if this signal component was primarily related to rotor static unbalance (i.e. radial force as function of square speed).

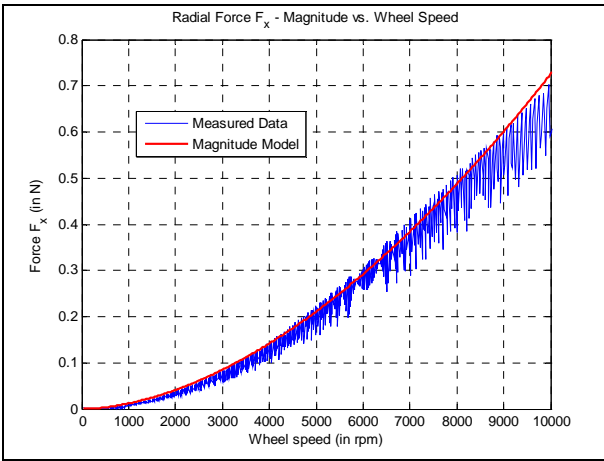


Figure 10: Magnitude Model for Order H1 Component

#### 4. THE IN-FLIGHT OPERATIONAL CASE

In most spacecraft, only regular equipment telemetry signals are acquired and monitored on a routine basis. Noise components related to mechanism performance may be indirectly found in such data, e.g. by analysing the instantaneous current of a DC motor (proportional to motor torque) in combination with other information, e.g. motor speed. However, the associated sampling rate is often well below 1 Hz, which does not allow for a mechanism noise investigation in a frequency range as considered in paragraph 3.

A direct measurement of mechanical noise quantities like accelerations or forces in directions, which do not relate to the primary actuation degree of freedom of a mechanism, would require additional sensors. The associated technical effort might be relatively high.

Nevertheless, in an experimental framework the equipment to measure microvibrations has been already

installed on several operational spacecraft, for instance the PAX experiment on OLYMPUS [6] and the Micro-Vibration Monitor (MVM) on ARTEMIS. Other investigations have alternatively used measurement data originating from an optical payload [9].

With a microvibration sensor installation at a single, centralised location of a spacecraft, there are several challenges for potential use in a health monitoring context:

- All equipment noise is effectively filtered by the structural transmission path from an individual source to the centralised receiver, specifically due to the mechanism's internal structure, the spacecraft main structure and any further elements contributing to the total transfer function.
- The received signal is a mixture of the noise received from all sources simultaneously.

In the following paragraphs, some examples of in-orbit mechanical noise measurements shall illustrate the problem.

#### Example 1:

Samples of PAX data acquired in March 1993 have been analysed, with primary focus on identifying noise signatures that can be associated with the reaction wheel assemblies of the OLYMPUS spacecraft. The PAX hardware comprised three accelerometers (x/y/z-axes), with a system bandwidth from 0.5 to 1000 Hz [6].

Time history windows of 20 seconds length have been processed. The power spectral densities of the non-calibrated acceleration signals (in arbitrary units, a.u.) for x-, y- and z-directions are plotted in *Figure 11*, already scaled as order spectra. The noise signature of a reaction wheel running at approx. 520 rpm has been identified by searching the spectra for harmonic sets.

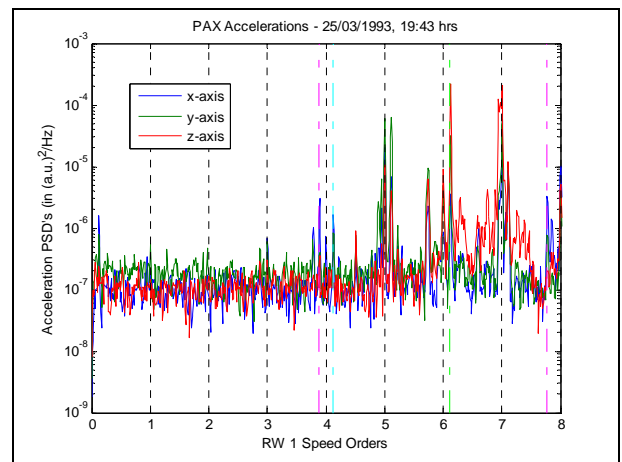


Figure 11: PAX Data - Order Spectra (RW 1, Day 1)

When plotting the spectra over wheel speed orders for the selected reaction wheel, the presence of significant tonal components at integer orders (marked by vertical dashed lines) has been confirmed.

Furthermore, characteristic non-integer orders related to the ball bearings as predicted e.g. according to [2] and [7] have been identified:  $H3.89$ ,  $H4.13$ ,  $H6.11$  and  $H7.78 = 2 \times 3.89$ . They are highlighted by vertical dash-dot lines. Moreover, there are other tonal components in the signal, which are not caused by the reaction wheel considered.

The identification of tonal noise components has been repeated for other data sets. This has allowed for order tracking, while the speeds of the reaction wheels were changing due to spacecraft attitude control. Figure 12 represents the identification results for the signature of the same reaction wheel as selected above, however approximately 19 hours later, and taking into account that the wheel speed had increased to about 870 rpm in the meantime.

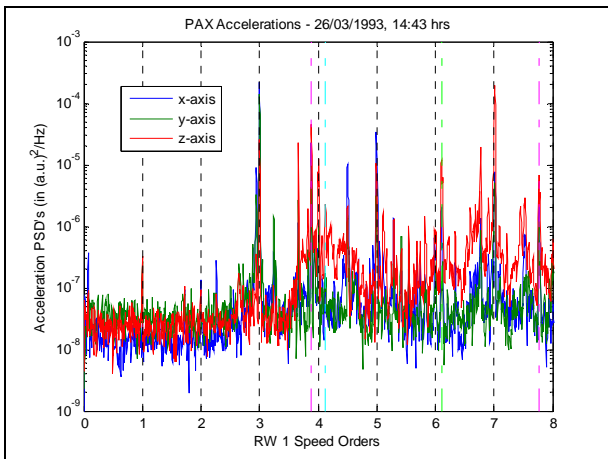


Figure 12: PAX Data - Order Spectra (RW 1, Day 2)

By a closer inspection of the broadband noise, it can be noticed that several features have been left-shifted in the order spectra. However, the reliability of tracking the correct noise signature has been particularly increased by re-identifying the very typical features at  $H3.89$ ,  $H4.13$ ,  $H6.11$  and  $H7.78$  closely related to the geometry of the ball bearings used in the reaction wheel assembly.

Further scanning for harmonic sets has revealed the signature of a second reaction wheel running at about 1970 rpm, see Figure 13. However, the ball bearing related features at  $H3.89$  and  $H4.13$  are very difficult to distinguish from the background noise.

The interpretation of magnitudes of particular features in the noise signatures will require further research taking, among others, the transfer function effects of the different noise propagation paths into account.

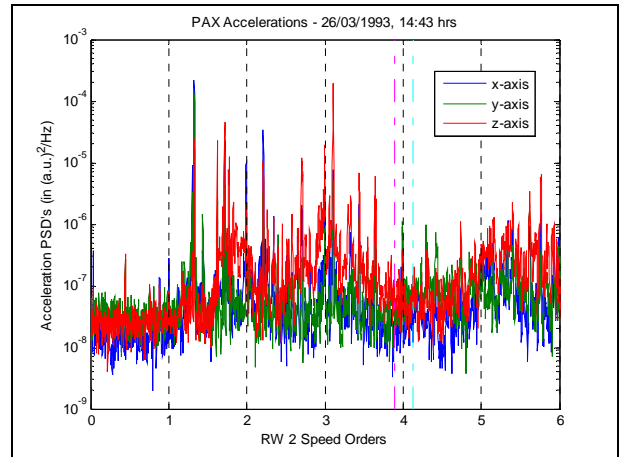


Figure 13: PAX Data - Order Spectra (RW 2, Day 2)

### Example 2:

For the characterisation of microvibrations that could potentially disturb the optical communication terminal SILEX onboard the ARTEMIS spacecraft, a dedicated Micro-Vibration Monitor (MVM) was installed on the spacecraft. The on-ground investigations for ARTEMIS regarding microvibration sources and structural effects are summarised in [8].

Figure 14 shows the spectrogram of an acceleration time history (MVM channel 0) sampled at 2 kHz over 54 seconds during the early phase of the spacecraft mission.

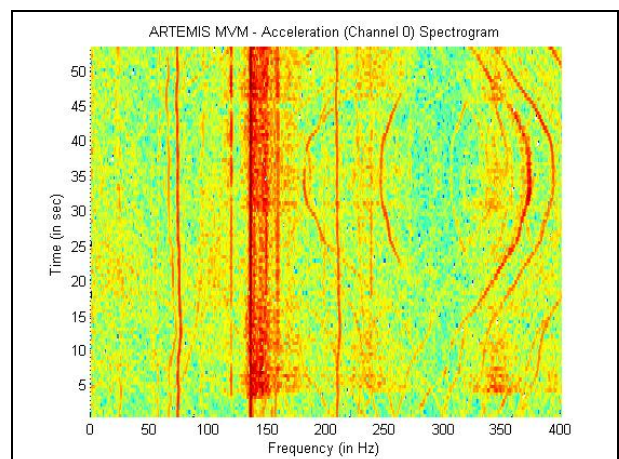


Figure 14: MVM Acceleration Data - Spectrogram

The attitude control subsystem of ARTEMIS includes two reaction wheels operating in a speed range of  $\pm 2700$  rpm and two momentum wheels with a bias speed in the range 3200 to 5400 rpm.

While the speed of the reaction wheels may rapidly change, the momentum wheels normally stay at almost constant speed over longer periods of time.

The spectrogram in *Figure 14* highlights spectral peak magnitudes over time in form of distinct lines. It can be seen that certain features stay approximately constant in frequency (vertical lines), whereas other features show large frequency changes over time.

As an example, the spectral line at about 74 Hz has been associated with the basic harmonic *HI* of one momentum wheel running at a speed of about 4440 rpm. The sine-like features at higher frequencies are probably related to upper harmonics in the noise signatures of the reaction wheels going quickly up and down in speed.

In addition, the spectrogram reveals some non-stationary components in the overall signal, for instance some broad-band transient events at about 5 seconds of the time scale, which are likely caused by other mechanisms onboard the spacecraft.

## 5. CONCLUSIONS AND OUTLOOK

Via selected examples of signal acquisition during ground testing and in-orbit monitoring, first steps of detecting, classifying and estimating mechanism noise components have been discussed.

Further research aiming at concepts for space mechanism health monitoring is planned, with emphasis on the following tasks:

- Collection of representative noise signatures from relevant mechanism equipment during ground testing,
- Development of robust algorithms for automated feature extraction and change detection, and
- Development of advanced noise models and their correlation with test data for different space mechanisms, and a more detailed consideration of physical causes for specific features in noise signatures.

## 6. ACKNOWLEDGEMENTS

The authors gratefully acknowledged that all measured data and related information on test items and facilities used for the investigation have been kindly made available by different ESA projects.

## 7. REFERENCES

- [1] Laurens, Ph., Dupuis, P.-E., Phillips, N. & Kugel, U.: Noise Identification Models and Benchmark Testing of Mechanisms. Proc. 2<sup>nd</sup> Space Microdynamics and Accurate Control Symposium, Toulouse, France, May 1997.
- [2] Laurens, Ph. & Decoux, E.: Understanding and Monitoring Space Mechanisms through their Microdynamic Signature. ESA SP-410, Proc. 7<sup>th</sup> European Space Mechanisms and Tribology Symposium, ESTEC, Noordwijk, The Netherlands, Oct. 1997, pp. 183-189.
- [3] Laurens, Ph. & Decoux, E.: Microdynamic Behaviour of Momentum and Reaction Wheels.
- [4] Dyne, S.J.C.: Remote Vibration Monitoring. Measurement + Control, Volume 26 no. 9, Nov. 1993.
- [5] Ferguson, N.S., Pinder, J.N. & Tunbridge, D.E.L.: Spacecraft Vibrations due to Mechanisms; Measurements from Olympus On-station. Proc. 5<sup>th</sup> European Space Mechanisms & Tribology Symposium, ESTEC, Noordwijk, The Netherlands, Oct. 1992, pp. 221-227.
- [6] Tunbridge, D.: The 'PAX' Experiment on Olympus. ESA Bulletin No. 64.
- [7] Technical Memorandum ESTL/TM/133: A Review of the Influence of Bearing Noise on the Microgravity/Microvibration Environment of Spacecraft. ESTL, March 1994.
- [8] Galeazzi, C., Marucchi-Chierro, P.C. & Holtz, L.V.: Experimental Activities on ARTEMIS for the Microvibration Verification. ESA SP-386 Proc. Conference on Spacecraft Structures, Materials & Mechanical Testing, Noordwijk, The Netherlands, June 1996, pp. 997-1006.
- [9] De Gaujac, A.C., Monteil, D., Bousquet, C.: In Orbit Microvibration Test on SPOT 1 Satellite – Experiment Principle and Results. ESA SP-323, Proc. 1<sup>st</sup> ESA International Conference on Spacecraft Guidance, Navigation and Control Systems, ESTEC, Noordwijk, The Netherlands, Dec. 1991.
- [10] Wowk, V.: Machinery Vibration – Measurement and Analysis. McGraw-Hill Inc., New York, 1991.
- [11] Vibration Measurement. Company Publication, Brüel & Kjær, Denmark.